A molecular dynamics study on thermal and mechanical behavior of graphene-copper nanocomposites for automobile & aerospace industry

Q. Anjam[a] , F. Hussain[b], M. Imran[a,*], N. Amin[a,], M. Kashif[a]
[a]*Physics Department, Govt College University Faisalabad (GCUF), Allama Iqbal Road, Faisalabad 38000, Pakistan*
[b]*Materials Simulation Research Laboratory (MSRL), Department of Physics Bahauddin Zakariya University Multan Pakistan*

The effect of graphene copper (GN/Cu) nanocomposites interface is the main factor to understand glides and shuffles dislocations which significantly affect the thermo-mechanical performance of graphene copper nanocomposites for ultra high strength materials applications in the automobile & aerospace industry. Here, we report the recital optimization of graphene interaction with copper by molecular dynamics (MD) simulation. To analyze the effect of temperature and stress three various orientations of Cu ((1 0 0), (1 1 0), and (1 1 1)) have been chosen. The nanocomposites were heated from 300k-1500k to predict the melting temperature by mean square displacement (MSD) and radial distribution function (RDF). Apart from interface, edges in graphene can also cause dislocations nucleation. Furthermore, GN/Cu nanocomposites have been subjected to uniaxial tensile loading along with armchair and zigzag directions. The stress-strain curves were used to calculate mechanical strength by comparing them with pure copper counterparts. The melting temperature of GN/Cu (1 0 0), GN/ Cu (1 1 0), and GN/ Cu (1 1 1) have been observed from MSD are 1191k, 1053k, and 1332k respectively. The lowest melting temperature of GN/ Cu (1 1 0) shows its unstable structure due to a greater lattice mismatch. GN/ Cu (1 1 1) has a higher melting temperature as compared to GN/ Cu (1 0 0) and GN/ Cu (1 1 0) due to less phase transformation and propagation of shuffle dislocations. The stress of pure copper has been observed as 5.9 Gpa along the armchair direction. It was observed from stress-strain curves under a constant strain rate of 5×10^{9} along the armchair direction, the values of stress for GN/ Cu (1 0 0), GN/ Cu (1 1 0), and GN/ Cu (1 1 1) were calculated 22.5 Gpa, 21.9 Gpa, 26.8 Gpa respectively. Moreover, it was calculated that the mechanical strength of GN/Ag (1 0 0), GN/ Cu (1 1 0), and GN/ Cu (1 1 1) increased by 381.3%, 371.1%, 454.2% along the armchair direction as compared to pure copper. It was found that the values of stress along zigzag direction for pure Cu, GN/ Cu (1 0 0), GN/ Cu (1 1 0), and GN/ Cu (1 1 1) were calculated as 2.1 Gpa, 25.4 Gpa, 21.0 Gpa, 31Gpa respectively. It was investigated that the strength of GN/ Cu (1 0 0), GN/ Cu (1 1 0), and GN/ Cu (1 1 1) increased by 1209.5%, 1000%, 1476.1% as compared to pure copper along the zigzag direction. Based on the above-mentioned results, GN/Cu nanocomposites can be used in the automobile& aerospace industry in next future applications.

(Received May 25, 2021; Accepted September 15, 2021)

Keywords: Nanocomposites, Graphene copper, Deformation, Melting point, Thermodynamic stability

1. Introduction

GN metal nanocomposites have attracted much attention due to interface as well as dislocations because they are in progress of ultra high strength materials applications for the automobile and aerospace industry. Moreover, graphene incorporation with copper not only improves mechanical performance but also design function which is useful in various applications of engineering. Furthermore, researchers have fabricated graphene metal nanocomposites along with the various degree of reinforcement of hardness, strength, and elastic modulus by using compression tests. Graphene is a unique two-dimensional material consists of sp^2 hybridized

* Corresponding authors: imraniub86@gcuf.edu.pk

carbon atoms packed into a honeycomb crystal lattice because of its extraordinary properties as larger surface area (2630)m^2 [1], extremely apparent to visible light (~2.3% amalgamation) [2], maximum thermal conductivity (~5000 $Wm^{-1}K^{-1}$) [3], outstanding mechanical strength (young's modules ~1.1TPa) [4]. The copper metal is used in industrial machinery and graphene is a one atom thick layer. These two are the best contenders due to significant thermo-mechanical performance not only in aerospace but also in the automobile industry. Many graphene metal nanocomposites are commercially synthesized to improve the thermo-mechanical performance of these materials in the automobile industry to make stronger vehicles and in the aerospace industry for sporting goods as well as aerospace constituents. These nanocomposites are used to make various parts of passenger aircrafts such as doors, spoilers, fairings, and elevators to increase fuel efficiency and reduced weight [5]. Furthermore, it is necessary to use lightweight, low cost and long-life nanocomposites. These nanocomposites are used in favors over polymers composites due to lightweight, thermally stable to restrained high temperature (1000 c^0) applications and ultrahigh mechanical strength [6].

It has been shown that graphene copper nanocomposites got novel thermal characteristics because of their low mass and the strongest bonding of carbon atoms [7]. The tensile strength and fracture strain decreased by increasing the temperature or size of the graphene copper nanocomposites [8,9]. It has been observed that a hole in graphene copper exhibits complex behavior at a boundary that improves stability due to the low dimensional interface [10]. The lattice defects and density significantly improve the stability, stiffness as well as strength of graphene copper nanocomposites [11]. Salam et al. synthesized GN/Cu nanocomposites due to inexpensiveness, superior catalytic properties which were reused five times without a reduction in selectivity [12]. With the rapid progress and development in the aerospace industry, the accessible technologies developed do not have enough potential to overcome the demands and development of the innovative era. Nanocomposites based on CNT have procured comprehensive concentration in recent years intended for their applications in, military crafts, aircraft, spacecraft, and missiles owing to superior properties such as thermal stability, mechanical strength, and huge surface area. S.K Bhunia et al. devolved reduced GN/Cu nanocomposites which control pollution that acts as the best photocatalyst under visible light [13]. GN combined with various metals like Al, Ag, Cu, and Au significantly improve the strength, hardness, fracture, and modules of elasticity [14-17].

The major objective of the recent work is to study the improvement of the thermo-mechanical performance of graphene copper nanocomposites in the automobile industry and aerospace applications. The incorporation of graphene metal nanocomposites in the automobile and aerospace industry has got incredible attention starting from the structural behavior of materials, mechanical strength, and design applications. The major reason for the incorporation of graphene copper nanocomposites is to provide cheaper, safer transportation in the aerospace industry. To control the phase transition and structural organization between GN/Cu nanocomposites is the non-bonded interaction energy [18]. GN/Cu nanocomposites are extremely exceptional materials with high thermal stability used for the development of flexible electronic circuits and as a catalyst due to the unique FCC structure of Cu [19]. It has been observed that GN/Cu nanocomposites due to the hexagonal structure of graphene considerably affect thermal properties [20]. Despite many concerning metal matrix composites reported in experimental studies, only a few studies offer regarding GN metal composites by MD simulation [21]. Amel et al. investigated the evolution and distribution of atomic nanoclusters of tinny material over the GN substrates such as Ag, Cu that formed aggregates of different sizes [22]. Moreover, it has been developed that GN/Cu nanocomposites improve mechanical properties based on fracture strain, tensile strength, and young's modules [23]. Khan et al. synthesized GN/Cu nanocomposites experimentally which improve electrical conductivity and photoelectrochemical performance [24].

The present work is performed to examine the thermal and mechanical behavior of GN/Cu nanocomposites by using MD simulation. The Large-scale Atomic/Molecular Massively Parallel Simulator (LAMMPS) [25] package was used to perform all simulations throughout the work. All snapshots were taken with the use of visual molecular dynamics (VMD) code [26]. In the present simulation, adaptive intermolecular reactive empirical bond order (AIREBO) [27] potential was used for interactions between C-C atoms. It includes an adaptive behavior of the dihedral angle, non bonded, and torsional interactions, which still allow unfixed hybridization state for covalent

bonding interactions and effectively simulates covalent bond formation, breaking, and orbital hybridization of atoms [28]. Furthermore, the accuracy of the MD simulations depends on the type of force field used to simulate the sample. The AIREBO [29] inter-atomic force field yields close to results of higher-order density functional theory (DFT) studies most widely used for simulated GN, carbon nanotubes (CNTs), and related two-dimensional materials (2D) [30]. The outcomes of this study provide a comprehensive understanding of the structural stability, interfacial strength, propagation of dislocations, and deformation mechanism in graphene copper nanocomposites which increases the performance of these materials in the automobile& aerospace industry.

2. Simulation Methodology

Firstly build a cubic cell of Cu with different orientations as pure Cu, Cu (1 0 0), Cu (1 1 0), and Cu (1 1 1) with a lattice constant 3.615 Å of Cu considered as a substrate with a length of the cell in x, y, z direction in different orientations (±40Å, ±40Å, ±18.3Å) containing 1264 atoms. The size of single-layer graphene (SLG) sheet in x, y, and z-direction was (±40Å, ±40Å, ±15.5Å) containing 627 atoms of graphene with a lattice constant of 2.46 Å. One atom thick SLG (having hexagonal structure) sheet was packed on the top surface of copper. MD simulations consist of the following steps. Firstly copper equilibrated at a fixed temperature (10k-300k) for achieving an equilibrium state at 0.001ps. The experimentally determined Cu melting temperature was 1358K. That's why a comparatively higher temperature of 1500k was selected to achieve a homogeneous disorder of the copper. The SLG can with a stand at 3300k estimated by MD and 2073k estimated experimentally. Secondly, SLG laminated over Cu in various orientations, the composites heated as well as simulated from 300k to 1500k. The earlier studies specified that carbon bonds need rotation and stretching during the process of ring formation or defects of heating. The superior temperature increases the kinetic energy to assist the composites. MD simulations were performed at different temperatures initially 10k to 10 K, then 300k to 300k, and finally 300 to 1500k respectively. It is observed that molecules of the graphene possibly will not decompose at low temperatures. In the previous studies, the decomposition of the hydrocarbon molecules was not under consideration. It has been observed that the melting temperature significantly affects the thermal properties of the nanocomposites. At very high temperatures the substrate surface can destroy or yet the graphene lattice. MD simulations were carried out with a constant number of atoms, pressure, temperature ensemble (NPT). Throughout the work, periodic boundary conditions were applied in all directions. A conjugate gradient method was used to relax and minimize the energy of atoms in graphene copper nanocomposites. The system was then allowed to equilibrate using the Nose-Hover thermostat at 300k for 1×10^{-9} s.

2.1. Interatomic Potentials

A computational model was used containing two types of atoms such as copper (Cu) and carbon (C). Different kinds of potentials were used for different interactions during the whole simulation. For Cu-Cu atoms interactions, the embedded atom method (EAM) potential was used for the calculation of potential energy between metal atoms and its equation is

$$E = \sum F_i(\sigma_{ij}) + \frac{1}{2}\sum_i \sum_j (\emptyset)_{ij}(R)_{ij} \quad (1)$$

where $F_i(\sigma_{ij})$ is the electron density embedded energy and $(\emptyset)_{ij}$, $(R)_{ij}$ is the repulsive interaction between core atoms. One must know the host atoms' embedded energy and repulsive force between cores in MD simulations. This potential is mostly used for the thermal and mechanical properties of metals and alloys. To approximate the interaction between two neutral atoms or molecules Lenard-Jones (L-J) potential was used in MD simulations. The L-J potential used for the calculation of non-bonded interaction energy between Cu and C atoms and its equation is given as

$$V_{lj} = 4\varepsilon[\left(\frac{\sigma}{r}\right)^{12} - \left(\frac{\sigma}{r}\right)^{6}] \quad (2)$$

Here σ is the finite distance at which interparticle potential zero and is **ε** the potential well depth. The term r is the distance between particles. The terms **ε** and σ depend on the material characteristics that physically describe adhesiveness and lubrication properties. The potential parameters for graphene copper nanocomposites were taken as

$$\varepsilon_{Cu-C} = 0.02578\text{ev} \tag{3}$$

$$\sigma_{Cu-C} = 3.0825\text{Å} \tag{4}$$

where the value of **ε** is in the range of (0.01-0.05ev) for generalizing interface characteristics of the GN/Cu nanocomposites.

3. Results and Discussion

The propagation of dislocations plays an important role in the melting as well as deformation mechanism which significantly affects the thermo-mechanical performance of nanocomposites in the automobile and aerospace industry [31]. Furthermore, the interface also has a significant effect on thermo-mechanical performance based on the dislocation nucleation [32]. In the first section, the dynamic melting behavior of graphene copper nanocomposites is studied by heating from 300k to 1500k. The MSD and RDF are used to estimate the melting temperature which improves the thermal stability of graphene copper nanocomposites. In the second section, mechanical strength was estimated by uniaxial tensile loading along armchair and zigzag directions to inspect the modulus of elasticity which enhances the mechanical performance of graphene copper nanocomposites.

3.1. Thermal Properties

In the recent development of the automobile & aerospace industry, efficient heat dissipation plays an important role which requires thermal stable materials with low conductivity, coefficient thermal expansion (CTE), and thermal conductivity (TC). GN/Cu nanocomposites attracted much attention due to the best thermal stability in various fields such as sensors, the automobile industry, and thermal management systems for aerospace applications.

In the present research to compare and calculate melting temperature, we computed MSD and RDF for structural thermodynamical stability of the material. It has been shown from figure.1 that the melting temperature is sensitive to orientations. Firstly, all samples were heated at 10k to equilibrate the composites and then the composites were melted at 300-1500k temperatures. Initially, it was observed that the response of the heating process for all samples remained the same. However, after some time a point was reached when GN/Cu (1 1 0) started deformation more quickly as compared to other samples which showed the lowest melting temperature of 1150k. The calculated temperatures for GN/Cu (1 0 0), GN/Cu (1 1 0), and GN/Cu (1 1 1) are 1191K, 1053K, and 1332K as shown in figure.1. The temperature vs MSD has been shown at different time steps in figure.1. The lowest temperature 1053k of GN/Cu (1 1 0) showed a more lattice mismatch and unstable structure due to which MSD increased. It can be observed from figure.1 that GN/Cu (1 1 1) has higher melting temperatures due to less phase transformation. It means that this is a more thermodynamically stable structure of graphene copper nanocomposites. The different snapshots were taken with visual molecular dynamics (VMD) as shown in figure.2.

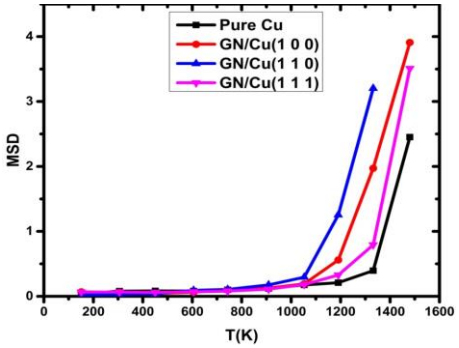

Fig. 1. Comparison of MSD vs temperature of pure Cu, GN/Cu (1 0 0), GN/Cu (1 1 0), and GN/Cu (1 1 1).

The reactive edges of graphene form a covalent bond with the neighboring graphene atoms which produces a unique network in the graphene copper nanocomposites system as shown in figure.2. The MSD of graphene copper nanocomposites was calculated to quantify the atomic mobility during equilibration at 10k and heating from 300k-1500k as shown in figure.2. However, the mixing of very reactive graphene edges forms a covalent bond with the nearest graphene to minimize the energy of the system. As shown from the figure (B) a more number of octagons were produced on the left side of the GN/Cu (1 0 0) sample whereas on the right side on the graphene layer for GN/Cu (1 1 1). It can be seen in figure (C) that octagon and pentagon both produced shuffle dislocations during the melting process for GN/Cu (1 1 0) which improves the thermal properties of the material. It has been observed that pinned dislocations are produced when more number broken bonds between carbon atoms of graphene and new bonds are formed randomly. These dislocations improve the thermal performance of the material that affects significantly thermal properties.

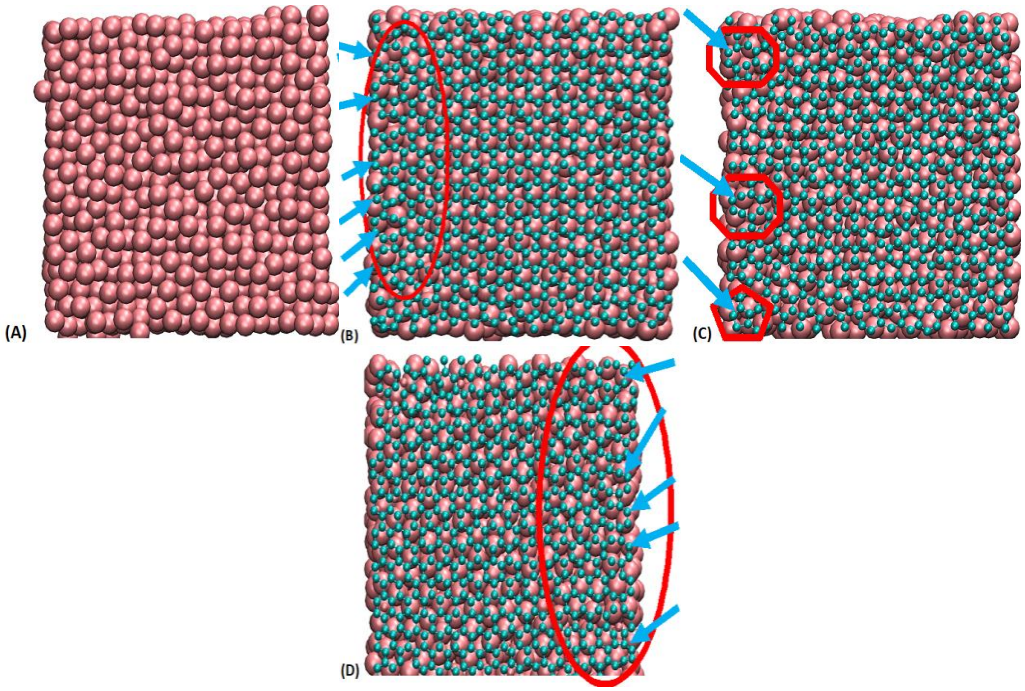

Fig. 2. Melting behavior of (A) pure Cu, (B) GN/Cu (1 0 0), (C) GN/Cu (1 1 0) and (D) GN/Cu (1 1 1).

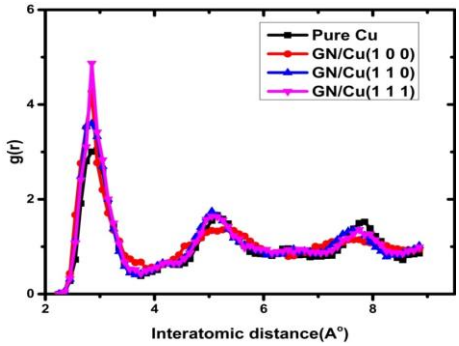

Fig. 3. Graph of RDF and interatomic distance of pure Cu, GN/Cu (1 0 0), GN/Cu (1 1 0), and GN/Cu (1 1 1).

RDF curves are plotted against interatomic distance to check the structural stability of Cu and graphene copper nanocomposites. To compare and calculate the melting temperature, we computed the RDF of all samples. It has been shown from figure.3 that the behavior of the heating process is different for all samples. At the start all the samples have shown quite similar behavior, however, a point reached where the nanocomposites start deformation due to different metal orientations. It has been shown from figure.3 that the first peak of crystalline pure Cu is at 2.5 Å and the next peaks are less due to an unstable structure. It was observed that GN/Cu (1 0 0) with red color shows clear peaks at 300K, while at 1191K the sample peaks are wide and less. After this atoms must be disordered due to melting and the final configuration has fewer peaks because of unstable structure which gives valuable information of nanocomposites materials that affect the thermal properties. RDF of GN/Cu (1 1 0) shows that the first peak is clear while the next peaks were less wide at 1053K and the sample melted. The RDF graph of GN/Cu (1 1 1) at 300K temperature shows more and more compact peaks. The first peak appeared at 2.5 Å and the next peak at 1332K peaks were less and wide. The peaks were disappeared after the third peak and the line becomes smooth. It has been shown from figure.3 that GN/Cu (1 1 0) can be used to check the melting of other samples. The final structure of every sample was significantly different from each other. It means that the structure of GN/Cu (1 1 1) is relatively more stable which possesses a larger value of melting temperature. It was observed that structural disorder increased with orientations when RDF peaks become more indistinct. It has been observed that graphene single layer on copper substrate produce dislocation cores appears stable at high temperature that alter the configuration of nanocomposites edges. The unsatisfied and dangling bonds created in graphene i.e. formation of a heptagon, pentagon, and octagon which created glides and shuffle dislocations that significantly affect the thermal properties of the graphene copper nanocomposites.

4. Mechanical Properties

GN metal nanocomposites have been shown great interest due to interface as they were pitch in the progress of sensors, catalysis, nanoelectronic devices, hydrogen storage devices (Fonseca et al). Kim et al. observed the ultra-high strength of GN metal nanocomposites by the compression test. Duan et al. have been calculated the results related to the mechanical properties of GN-embedded metal nanocomposites by MD simulations due to the effect of GN layers and chirality. The bottom layer of Cu was fixed and both sides of the nanocomposites remain rigid upon which forces were applied. All samples of graphene copper nanocomposites were first subjected to uniaxial tensile loading along with armchair and zigzag direction to calculate the stress and strain values that affect the mechanical properties of graphene copper nanocomposites.

4.1. Deformation along Armchair Direction

The resulting stress-strain curves of graphene copper nanocomposites under a constant strain rate of 5×10^{9} along the armchair direction have been displayed as shown in figure.4. Graphs

exhibit that initially stresses were directly proportional to strain and then stress was dropped at lower yield strength. The values of stresses were calculated as 5.9 GPa, 22.5 GPa, 21.9 GPa, 26.8 GPa for Cu, GN/Cu (1 0 0), GN/Cu (1 1 0), and GN/Cu (1 1 1) and all samples broke at different strain rate due to ductile nature of nanocomposites and stress drastically decreased in the plastic region. At different time steps when the load was applied along an armchair direction, different snapshots of composites of all samples were taken with VMD as shown in figure.5. Initially, when stress was applied, the sample stretched in the x-direction, and porosity was created which can be seen in other figures. After that Cu was start to break because Cu is brittle as shown in figures.5. The resulting stress-strain curves of all samples under a strain rate of 5×10^{9} along armchair were displayed as shown in figure.4.

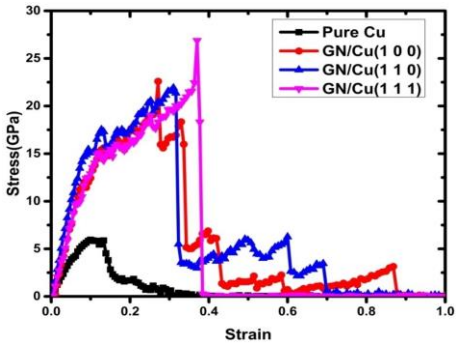

Fig. 4. Comparisons of stress vs strain curves of pure Cu, GN/Cu (1 0 0), GN/Cu (1 1 0), and GN/Cu (1 1 1) along the armchair direction.

Figure 4 shows the black curve for pure Cu, red for GN/Cu (1 0 0), blue for GN/Cu (1 1 0), and pink for GN/Cu (1 1 1) nanocomposites. The comparison of different sample curves shows that GN/Cu (1 1 1) breaks at 0.37 strains with larger stress 26.8 GPa and acts as more ductile material as shown in the figure.4. It has been shown from table 1 that the modulus of elasticity of GN/Cu (1 0 0) nanocomposite is larger as compared to other samples.

Table 1. The stress-strain comparision along the armchair direction.

Pure Cu & GN/Cu nanocomposites	**Stress (GPa)**	**Strain**	**Modulus=stress/strain Of elasticity**
Cu	5.9	0.10	5.9/0.10=59
GN/Cu (1 0 0)	22.5	0.27	22.5/027=83.3
GN/Cu (1 1 0)	21.9	0.30	21.9/0.30=73
GN/Cu (1 1 1)	26.8	0.37	26.8/0.37=72.4

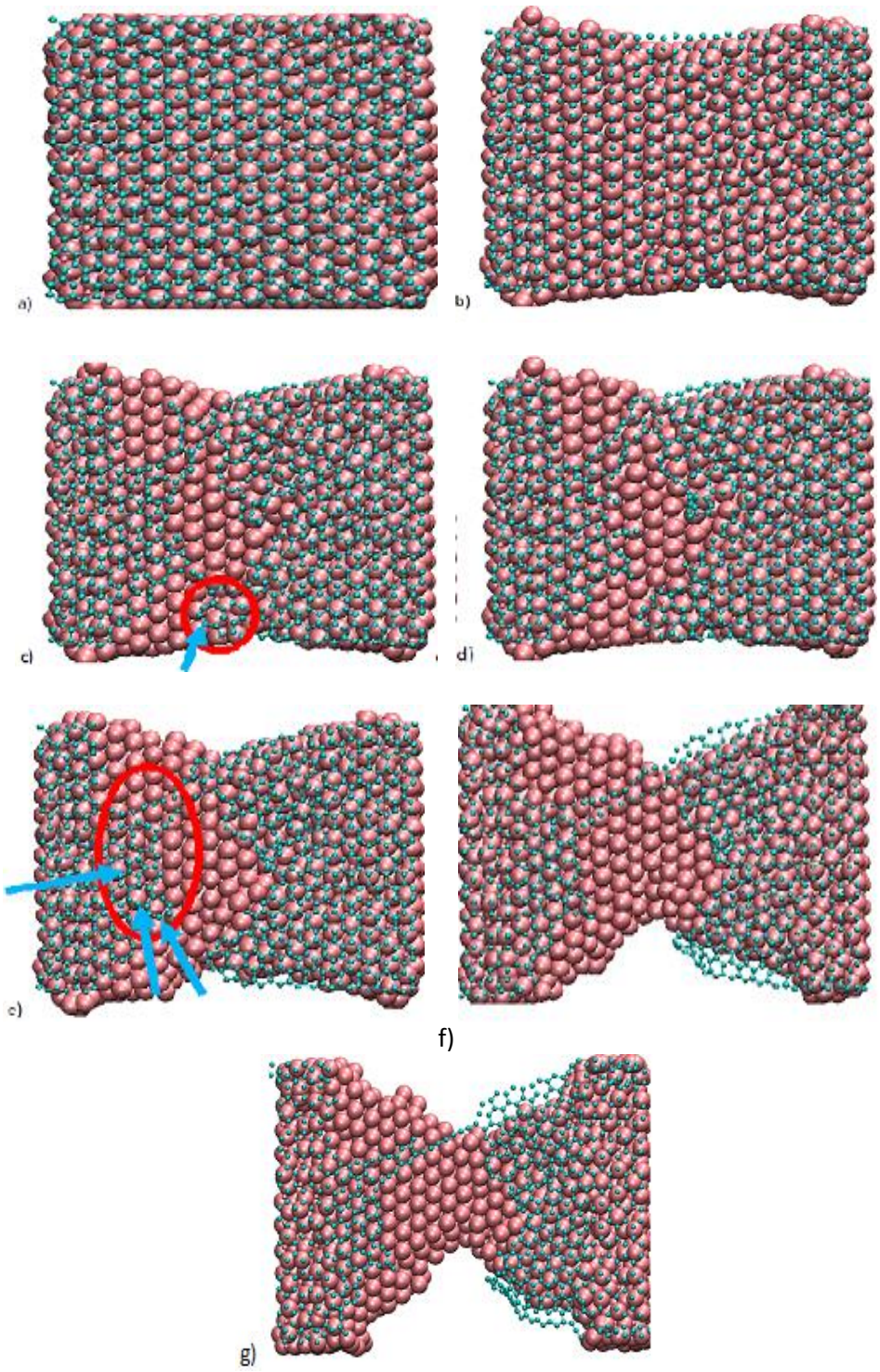

Fig. 5. Presenting (a,b,c,d,e, f,g) deformation behavior of GN/Cu (1 1 1), during uniaxial tensile loading along the armchair direction.

The snapshots of fig.5 have been shown the deformation of GN/Cu (1 1 1) nanocomposite at different time steps along with armchair directions. These snapshots were taken to describe the evolution of stress for all samples as a function of strain. After straining the composites, furthermore, the stress falls quickly to a smaller value singling the plastic deformation and loss of

strength of the nanocomposites. Since the nanocomposites were not fractured and then a smaller increase in stress is expected to continue increases with a constant strain rate. In the present work, two types of dislocations were observed under the deformation mechanism. The seven carbon atoms combined to form a heptagon and five carbon atoms combined to form a pentagon. The pair of heptagon and pentagon produces glide dislocations as shown in snapshots of figure.5.The glide dislocation generation increases which lead to the nanocomposites hardening that improves the strength of graphene copper nanocomposites. The eight carbon atoms are combined to form an octagon which produces shuffle dislocations. Based on these dislocations formation, the present research work is useful in many technical applications where a strong material is required. As shown in the above figures.5 (a, b), the graphene layer stretched then start breaking from both upper and lower sides. It has been shown in figures.5. (c) Heptagon formed shown by blue arrows inside the red circle. Figures.5. (e) shows that heptagons and pentagons produced glide dislocations which significantly affect the mechanical performance of the graphene copper nanocomposites. It has been shown with larger red circles in figures.5 (e), more than 7 number carbons atoms were combined. In figures.5 (c,d,e,f,g) the formation of vacancies and breaking of carbon atoms in a line as well as copper atoms started to break but one line of graphene atoms still not broke at the end of deformation process. It means that vacancies were created when the deformation rate increased along an armchair direction which significantly improved the mechanical performance of the graphene copper nanocomposites.

4.2. Deformation along Zigzag Direction

It has been shown from fig.6 that uniaxial tensile loading was applied along the zigzag direction and the nanocomposite unique deformation behavior was observed. It was observed that fracture started from the boundary with the breaking of a few C-C and Cu-C covalent bonds. The deformation behavior continues with an increasing strain rate. Deformation behavior was in excellent agreement with the higher-order quantum study of Yan et al. [33]. It has been observed that the values of strain rate and stress of GN/Cu (1 0 0) loaded along the zigzag direction are 0.27 and 25.4 GPa at the fracture point. The strain and stress values of GN/Cu (1 1 0) at the fracture point are 0.27 and 21.0 GPa. The strain and stress values for GN/Cu (1 1 1) at the fracture point are 0.39 and 31 GPa. The strain and stress values for the pure Cu at the fracture point are 0.04 and 2.1 GPa. It was observed that the sample GN/Cu (1 1 1) acts as more stable mechanically due to the larger value of strain and stress as shown in figure 6. It is evident from Fig. 6 that the graphene copper nanocomposites exhibit brittle deformation along the zigzag direction.

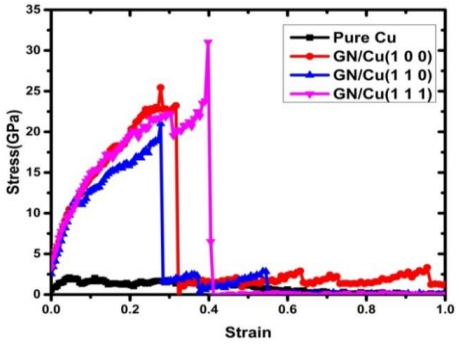

Fig. 6. Comparison of stress vs strain curves of pure Cu, GN/Cu (1 0 0), GN/Cu (1 1 0), and GN/Cu (1 1 1) along zigzag direction.

Figure 6 shows black curves for pure Cu, red for GN/Cu (1 0 0), blue for GN/Cu (1 1 0), and pink for GN/Cu (1 1 1) nanocomposites. The comparison of different sample curves shows that GN/Cu (1 1 1) nanocomposite break at 0.39 strain and ductile behavior as compared to other samples. This result is because of the less lattice mismatch between GN/Cu (1 1 1), as compared to other samples. As shown in the figures.7. (b,c,d,e,f,g) with larger size red circles the deformation along zigzag direction and layer of graphene starts breaking. It has been observed from figures (c,e,f,g) that pentagon, heptagon, and octagon produced both types of glide and shuffle dislocations. Finally, it was observed that when different combinations of carbon atoms formed as shown above which ultimately produced dislocations which increases the mechanical performance of graphene copper nanocomposites. It can be seen from Table 2, the modulus of elasticity of GN/Cu (1 0 0) nanocomposite is greater as compared to other samples.

Table 2.The stress-strain comparison along zigzag direction.

Pure Cu & GN/Cu nanocomposites	Stress (GPa)	Strain	Modulus=stress/strain Of elasticity
Cu	2.1	0.04	2.1/0.04=52.5
GN/Cu (1 0 0)	25.4	0.27	25.4/0.27=94.0
GN/Cu (1 1 0)	21.0	0.27	21.0/0.27=77.7
GN/Cu (1 1 1)	31	0.39	31/0.39=79.4

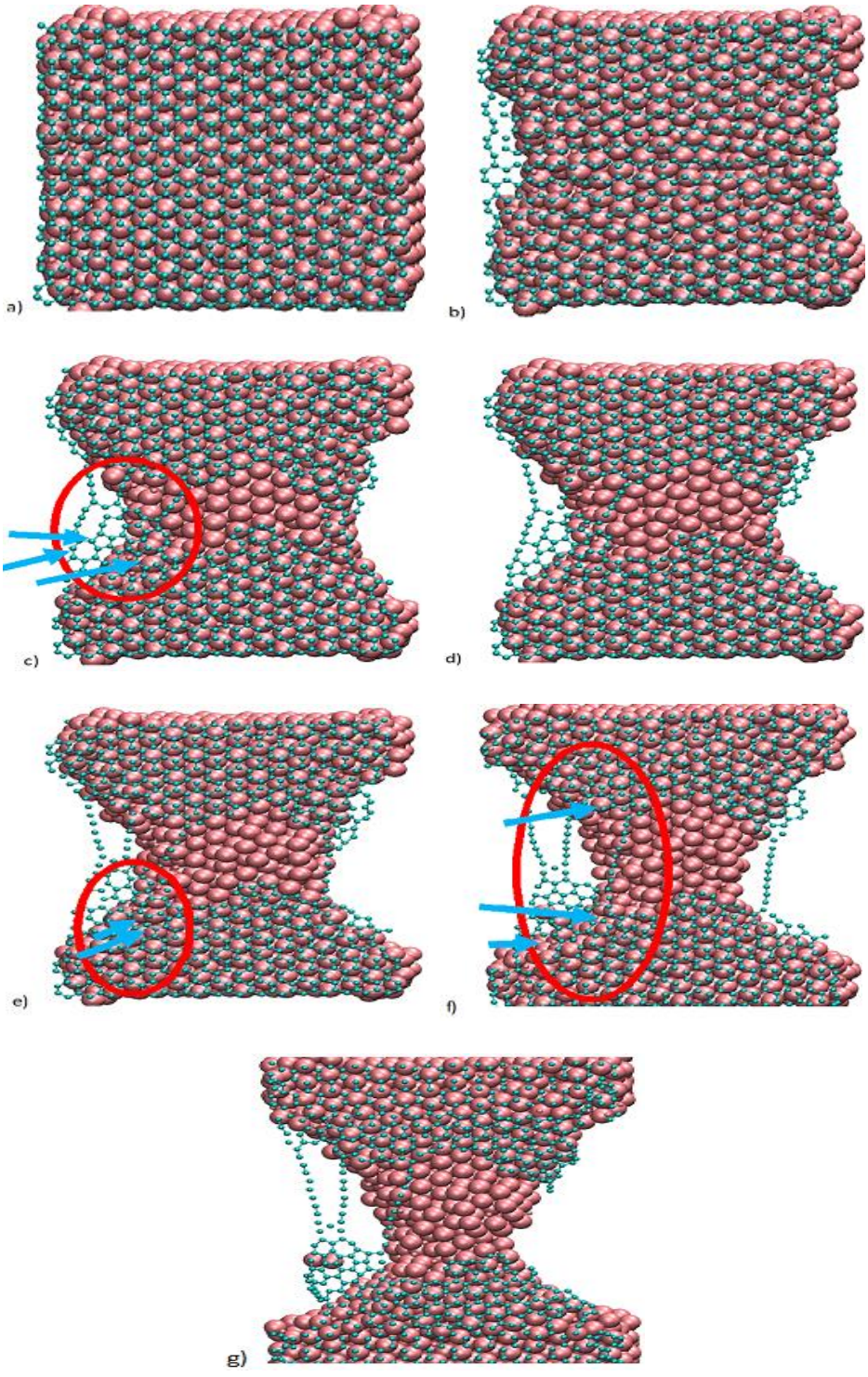

Fig. 7. Presenting (a,b,c,d,e,f,g) deformation behavior of best sample GN/Cu (1 1 1), during uniaxial tensile loading along the zigzag direction.

4.3. Deformation Comparison along with Armchair and Zigzag Direction

The Fracture behavior of both zigzag and armchair direction can be further analyzed by plotting to result in stress vs. strain data using the loading process. For a clear relationship between zigzag and armchair mode, resulting stress vs. strain curves can be compared and studied to predict their mechanical response of applied load. The resulting stress-strain curves for both zigzag and armchair of various samples have been presented. Initially, for both cases, stress is approximately directly proportional to strain. The strain and stress values for the pure Cu at the fracture point are 5.9 GPa at strain 0.10 along the armchair direction and 2.1 GPa at strain 0.04 along the zigzag direction. It was observed that the value of strain rate and stress of GN/Cu (1 0 0) along armchair direction are 0.27 and 22.5GPa at the fracture point. The value of stress is 25.4 GPa and strain 0.27 for GN/Cu (1 0 0) along the zigzag direction. The strain and stress values of GN/Cu (1 1 0) at the fracture point are 0.30 and 21.9 GPa along the armchair direction and 21.0 GPa at strain 0.27 along the zigzag direction. The strain and stress values of GN/Cu (1 1 1) at the fracture point are 0.37 and 26.8 GPa along the armchair direction and 31 GPa at strain 0.39 along zigzag direction. It is concluded that GN/Cu (1 1 1) is more stable mechanically due to the larger value of strain and stress in both cases along with armchair and zigzag direction. It was witnessed from the above-mentioned results that graphene copper nanocomposites exhibit ductile behavior along the armchair direction and brittle behavior along the zigzag direction.

Table 3.The stress-strain comparision along with armchair & zigzag direction.

Pure Cu & GN/Cu nanocomposites	Stress along with armchair (GPa)	Strain along the armchair direction	Stress along the zigzag direction (GPa)	Strain along zigzag dierection
Cu	5.9	0.10	2.1	0.04
GN/Cu (1 0 0)	22.5	0.27	25.4	0.27
GN/Cu (1 1 0)	21.9	0.30	21.0	0.27
GN/Cu (1 1 1)	26.8	0.37	31	0.39

5. Conclusions

In conclusion, the SLG sheet was successfully laminated on the Cu substrate to investigate the interface effect and production of different dislocations. To find out the thermal stability, structural stability, and intrinsic strength different Cu orientations were tried and the result shows, GN/Cu (1 1 1) nanocomposites are the most obvious stable structure. We have observed that glide and shuffle dislocation appear which increases the thermal stability of the material. Two types of glide and shuffle dislocations increase the strength of the GN/Cu nanocomposites. The results of the present work shed light on the melting and deformation mechanism in graphene copper nanocomposites which can be useful more efficient in the new fabrication and designing of graphene metal nanocomposites in automobiles & the aerospace industry.

We have also observed the difference in dislocations behavior due to graphene edges i.e. armchair and zigzag direction. Our present results have been shown that along zigzag orientations of the graphene copper nanocomposites have significant fracture strength and more stable structure of the material which considerably affect the mechanical properties. The comparison of stress-strain curves along armchair direction have been shown that GN/Cu (1 1 1) larger value of stress 26.8 GPa with a 0.37 strain rate and acts as more ductile material. The stress-strain comparison curves along zigzag direction have been shown a larger value of stress 31 GPa for GN/Cu (1 1 1) with 0.39 strain rate and act as a more brittle material. In the end, we have shown that interface and different dislocations improve the strength of the GN/Cu nanocomposites which can be useful in new designing as well as fabrication of graphene metal nanocomposites in the automobile & aerospace industry.

References

[1] Y. Shao, J. Wang, H. Wu, J. Liu, I. A. Aksay, Y. Lin, Electroanalysis: An International Journal Devoted to Fundamental and Practical Aspects of Electroanalysis **22**(10), 1027 (2010).
[2] R. R. Nair, P. Blake, A. N. Grigorenko, K. S. Novoselov, T. J. Booth, T. Stauber, A. K. Geim, Science, **320**(5881), 1308 (2008).
[3] L. A. Jauregui, Y. Yue, A. N. Sidorov, J. Hu, Q. Yu, G. Lopez, Y. P. Chen, Ecs Transactions **28**(5), 73 (2010).
[4] C. Lee, X. Wei, J. W. Kysar, J. Hone, Science **321**(5887), 385 (2008).
[5] K. C. Cheung, N. Gershenfeld, Science **341**(6151), 1219 (2013).
[6] L. Mei, Y. Li, R. Wang, C. Wang, Q. Peng, X. He, Polymers and Polymer Composites **19**(2-3), 107 (2011).
[7] K. Chu, F. Wang, Y. B. Li, X. H. Wang, D. J. Huang, Z. R. Geng, Composites Part A: Applied Science and Manufacturing **109**, 267 (2018).
[8] K. Duan, F. Zhu, K. Tang, L. He, Y. Chen, S. Liu, Computational Materials Science **117**, 294 (2016).
[9] Y. Ma, S. Zhang, Y. Xu, X. Liu, S. N. Luo, Physical Chemistry Chemical Physics **22**(8), 4741 (2020).
[10] M. Li, D. L. Cortie, J. Liu, D. Yu, S. M. K. N. Islam, L. Zhao, X. Wang, Nano Energy **53**, 993 (2018).
[11] K. Chu, J. Wang, Y. P. Liu, Z. R. Geng, Carbon **140**, 112 (2018).
[12] N. Salam, A. Sinha, A. S. Roy, P. Mondal, N. R. Jana, S. M. Islam, RSC Advances **4**(20), 10001 (2014).
[13] S. K. Bhunia, N. R. Jana, ACS applied materials & interfaces **6**(22), 20085 (2014).
[14] J. Wang, Z. Li, G. Fan, H. Pan, Z. Chen, D. Zhang, ScriptaMaterialia **66**(8), 594 (2012).
[15] S. F. Bartolucci, J. Paras, M. A. Rafiee, J. Rafiee, S. Lee, D. Kapoor, N. Koratkar, Materials Science and Engineering: A **528**(27), 7933 (2011).
[16] T. S. Koltsova, L. I. Nasibulina, I. V. Anoshkin, V. V. Mishin, E. I. Kauppinen, O. V. Tolochko, A. G. Nasibulin, Journal of Materials Science and Engineering B **2**(4), 240 (2012).
[17] L. Y. Chen, H. Konishi, A. Fehrenbacher, C. Ma, J. Q. Xu, H. Choi, X. C. Li, Scripta Materialia **67**(1), 29 (2012).
[18] S. Kumar, S. K. Das, S. K. Pattanayek, Computational Materials Science **152**, 393 (2018).
[19] C. T. Hsieh, Y. F. Chen, C. E. Lee, Y. M. Chiang, K. Y. Hsieh, H. S. Wu, Materials Chemistry and Physics **197**, 105 (2017).
[20] S. Weng, H. Ning, T. Fu, N. Hu, Y. Zhao, C. Huang, X. Peng, Scientific reports **8**(1), 1 (2018).
[21] S. Ali, F. Ahmad, P. S. M. M. Yusoff, N. Muhamad, E. Oñate, M. R. Raza, K. A. Malik, Composites Part A: Applied Science and Manufacturing **106357**, (2021).
[22] M. Amal Neek, R. Asgari, M. R. Tabar, Nanotechnology **20**(13), 135602 (2009).
[23] K. Chu, F. Wang, X. H. Wang, D. J. Huang, Materials Science and Engineering: A **713**, 269 (2018).
[24] M. E. Khan. M. M. Khan, M. H. Cho, New Journal of Chemistry **39**(10), 8121 (2015).
[25] B. Frantz Dale, S. J. Plimpton, M. S. Shephard, Engineering with Computers **26**(2), 205 (2010).
[26] W. Humphrey, A. Dalke, K. Schulten, Journal of molecular graphics **14**(1), 33 (1996).
[27] D. W. Brenner, Physical Review B **42**(15), 9458 (1990).
[28] S. J. Stuart, A. B. Tutein, J. A. Harrison The Journal of chemical physics **112**(14), 6472 (2000).
[29] G. Cao, Polymers **6**(9), 2404 (2014).
[30] G. Barbarino, C. Melis, L. Colombo, Carbon **80**, 167 (2014).
[31] D. U. Shanyi, Acta Materiae Compositae Sinica **1**, 000 (2007).
[32] J. Wang, Q. Zhou, S. Shao, A. Misra, Materials Research Letters **5**(1), 1 (2017).
[33] L. Yan, Y. B. Zheng, F. Zhao, S. Li, X. Gao, B. Xu, Y. Zhao, Chemical Society Reviews **41**(1), 97 (2012).